

Crystalline arrangements of microbubbles in monodisperse foams

Antje van der Net*, Gary W. Delaney, Wiebke Drenckhan,
Denis Weaire, Stefan Hutzler

School of Physics, Trinity College Dublin, Ireland

Received 5 September 2006; received in revised form 28 November 2006; accepted 29 November 2006

Available online 5 December 2006

Abstract

Monodisperse liquid foams consisting of equal-sized bubbles with diameters of a few hundred microns exhibit crystalline order, with a predominance of the fcc structure. This is inferred from observations at both bottom (foam–water) and top (foam–air) interfaces, together with supporting ray-tracing simulations. Diffusion of gas from the top layer into the atmosphere results in the formation of an ordered bidisperse top layer within a few minutes. In foam samples with a height of about 100 bubbles we have found a transition from mainly fcc packing at the (wet) bottom to the (bcc) Kelvin structure at the (dry) top. The issue of templating for the ordering in wet foams is addressed in soft sphere computer simulations.

© 2006 Elsevier B.V. All rights reserved.

Keywords: Foam; Crystalline structures; Fcc packing; Diffusion; Kelvin cells; Flow focusing; Terraces

1. Introduction

It is a surprising property of equal-sized bubbles in wet foams that they order almost perfectly in 3D, when deposited onto a pool of the surfactant solution from which they are made, as shown in Fig. 1. This was first observed by Bragg and Nye [1] (but never pursued any further by them [2]), using equal-size bubbles of diameter 100–700 μm . This is well below the capillary length l_0 , defined by

$$l_0^2 = \frac{\gamma}{\rho g}, \quad (1)$$

where γ is the surface tension; ρ the density of the liquid; g is the gravitational acceleration. For surfactant-based foams this length is about 1.6 mm. Foams consisting of such small bubbles remain wet (i.e. have a liquid fraction exceeding 20%) for a considerable number of layers of bubbles, which can be estimated as $N \simeq (l_0/d)^2$ [3]. In the experiments described in this paper, bubble diameters in the range from 250 μm to 400 μm were used, allowing us to create wet foams consisting of up to 25 layers of bubbles.

In wet foams the bubbles take on nearly spherical shapes, so this raises the question whether other systems, consisting of

particles of spherical shapes, also readily order. For macroscopic hard spheres (where thermal motion is negligible) this is not the case, unless very particular and controlled packing methods are used [4–6]. This was shown by Bernal, who also determined the packing fraction for a random close packed structure [7]. Hard sphere colloids (nanometer scale) are seen to readily order, but only at very long time-scales (days to weeks) [8,9]. When we consider foams or emulsions with bubbles larger than the capillary length, they do not readily order unless tightly confined [10–12] and/or by manually placing each bubble in the correct position [13]. Very little appears to be known on the spontaneous 3D ordering of macroscopic monodisperse emulsions, though the creation of monodisperse emulsion crystals using shear has repeatedly been reported [14,15] and might be of relevance here.

In the following we will first of all present a summary of recent results on the ordering of small bubbles in wet foams [3]. A detailed statistical analysis shows that packing is mainly in the fcc arrangement, consistent with the findings for some other ordered systems in nature [9,16,17]. Further work concerns the effect of coarsening of the top layer of bubbles, which leads to an intriguing sequence of topological transitions involving the first 2 layers. In tall columns of small bubbles, where the liquid fraction decreases with height due to gravitationally induced drainage, we find a transition to the Kelvin structure for dry foams. Finally we also present some preliminary computational results concerning the origin of the ordering in the wet limit.

* Corresponding author. Tel.: +353 1896 8453.

E-mail addresses: vanderna@tcd.ie (A. van der Net).

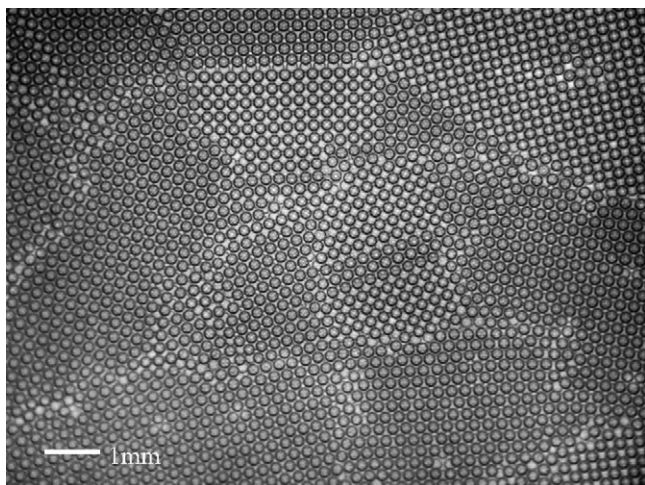


Fig. 1. View of the top of a pool of equal-sized bubbles (diameter $\sim 250 \mu\text{m}$), generated from aqueous detergent solution. This reveals different grains which are ordered according to familiar crystalline structures.

2. Formation and deposition of monodisperse microbubbles

In recent years an increased interest developed in the production of monodisperse microbubbles [18–21] and microdroplets, with applications in inkjet printing, drug delivery, microfluidics-based lab-on-chip technologies, optical devices and new insulation materials [19,22–27]. The favored technique, microfluidic flow focusing, is based on creating a co-flow of gas and liquid focused through a small orifice. This creates a gas jet which becomes unstable and breaks up into monodisperse microbubbles. The size of the bubbles is influenced by the characteristics of the gas and liquid flow and the orifice size [19,24], which in our case is less than $450 \mu\text{m}$ in diameter. In Fig. 2 the device used by us is shown. We use nitrogen and an aqueous solution of the commercial detergent Fairy Liquid[®] at 4% volume fraction (surface tension 28 mN/m).

When releasing the microbubbles directly from our foam generator onto a pool (diameter 13.5 cm), as shown in Fig. 2(b), we observe that they order easily into crystalline structures such as hcp and fcc. In Fig. 1 the top view of a bubble pool is shown, showing different crystal domains (grains) within the foam sample. We can release microbubbles from above the liquid pool ($5\text{--}10 \text{ cm}$), from below the water–foam interface, or even directly into the foam with the outlet slightly above it ($0.5\text{--}1 \text{ cm}$); in every case they form well ordered bubble crystals within the foam sample. In this article, all data is from samples created by releasing bubbles slightly above the foam sample. The samples are observed with a microscope from the top (see Fig. 2(c)), and from bottom, with the use of transmitted light.

3. Observations of order and defects

The observations of the top and the bottom of our foam samples show a variety of interesting crystalline structures and defects [3] of the type that can be found for example, in metal

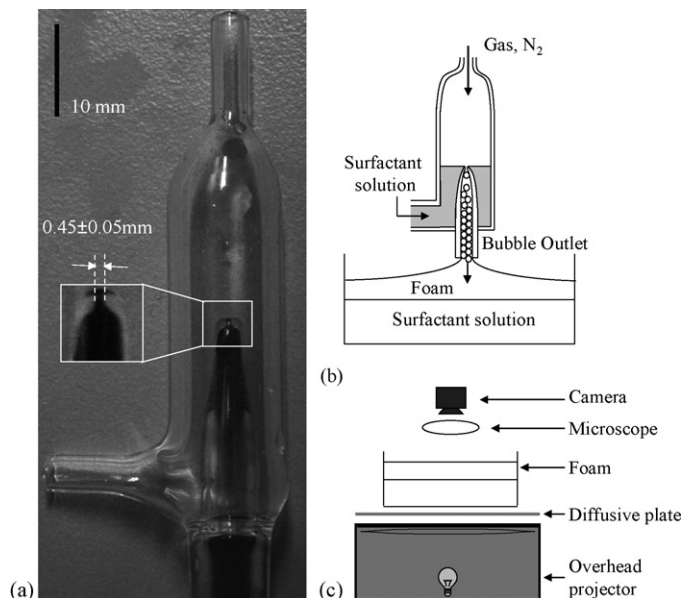


Fig. 2. Experimental set-up for the formation and imaging of monodisperse microbubbles. (a) Nitrogen gas flows into the device from the top, surfactant solution from the side. (b) At the orifice a co-flow of gas surrounded by water becomes unstable and breaks up into monodisperse bubbles. These are deposited onto a pool of surfactant solution. (c) The sample is viewed from top with transmitted light from an overhead projector.

structures. These may be identified by analysing several ordered layers of bubbles below the air–foam interface using ray-tracing techniques. We compare the experimental images with rendered images from the commercial animation software 3D Studio Max [28]. This software allows the user to input a sphere packing of a specified structure and in similar light conditions as in the experiment. Using the geometrical laws of optics and Fresnel's equations the software computes images of the sphere packings that can be compared with our experimental data.

In particular these simulations show us that the prominent black circles for each bubble should not be considered as the actual bubble perimeter, as shown in Fig. 1. The circles have a diameter slightly less than the bubble diameter, due to an optical effect [29].

The bubbles behave as divergent lenses refracting the pattern of the layers below. The effect of several layers is to create a fractal-like pattern as the final image. As is illustrated in Fig. 3, by considering the contribution to the observed patterns from the third layer of bubbles, the distinction can be made between the stackings ABC and ABA, which are consistent with the fcc(1 1 1) and hcp crystalline packings. The observed square patterns in Fig. 1 are consistent with an fcc(1 0 0) oriented crystalline structure.

Within the grains, we find imperfections such as stacking faults and surface defects, e.g. vacancies and divacancies [3]. The grain boundaries seen in Fig. 1 can be disordered or ordered. Ordered or *coherent* grain boundaries are only found between grains of two different oriented crystalline structures, in our case fcc(1 1 1) or hcp and fcc(1 0 0) oriented grains. Examples are shown in Fig. 4.

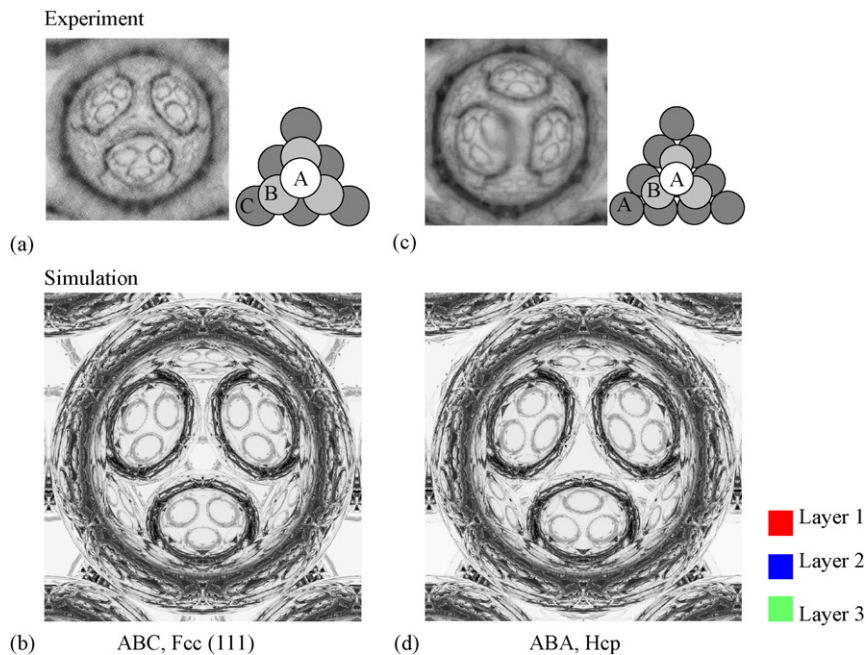


Fig. 3. Bubbles behave as divergent lenses which diminish and deform images of layers underneath them. The resulting pattern can be used to distinguish between ABC (a and b) and ABA (c and d) packed layers. ABC is consistent with the fcc(1 1 1) crystalline structure and ABA with the hcp structure. The simulations of 3D Studio Max [28] match well with the experimental observations.

Fig. 5 shows a view of the foam–water interface, where terraces can be clearly observed [3]. Just as at the top of the foam sample, one can see grain boundaries, stacking faults and dislocations. Occasionally we can follow them clearly within an extended sequence of terraces, as shown in Fig. 6. The observations of these terraces are an indication of ordering in the bulk. We analysed the terraces at the foam–water interface to obtain statistical data on the frequency of the occurrence of the different crystalline structures (Section 4).

4. Statistics of occurrence of crystalline structures

The bubbles of the lower layers contribute to the optical patterns observed when viewing the sample from top. This enables us to identify the ordering of the top three layers of bubbles and to investigate the occurrence of apparent fcc(1 1 1), fcc(1 0 0), hcp and ‘other’ structures. We have identified the type of ordering of the bubbles in 202 randomly chosen regions on the top of 28 different foam samples. Table 1 summarises

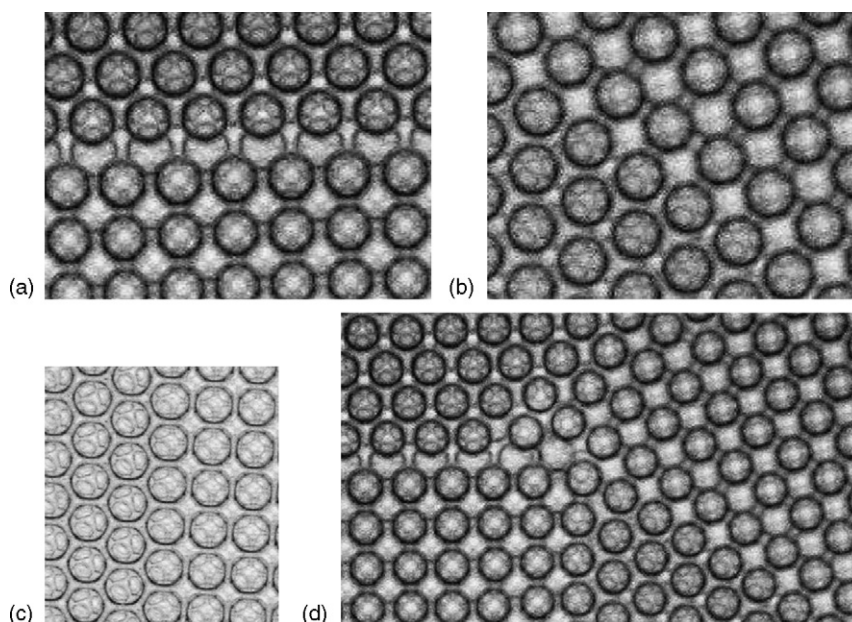


Fig. 4. Observed coherent grain boundaries. (a)–(c) are coherent grain boundaries between fcc(1 1 1) and fcc(1 0 0), known from metallurgy, (d) shows a junction of three coherent grain boundaries, posing a considerable puzzle as to its continuation into the bulk.

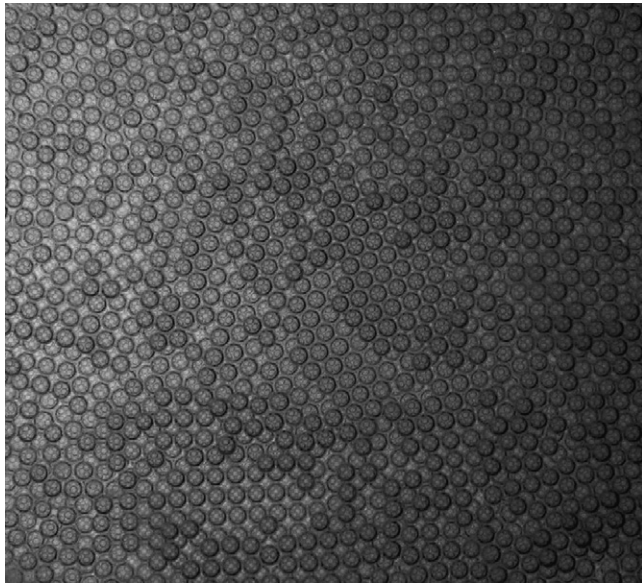


Fig. 5. A view of the foam–water interface (taken from below the sample) reveals terraces, which may be used to determine stacking sequences.

Table 1
Results for the structural analysis of 202 regions, chosen from random locations in the top layer of 28 foam samples

Type of ordering	Number of observations	Fraction
fcc(1 1 1) (ABC)	107	0.53
fcc(1 0 0)	12	0.059
hcp (ABA)	63	0.31
Undefined	20	0.099
Total number of observations	202	1.0

Table 2
Structural analysis of the terraces (of four layers or more) at the foam–water interface

Type of ordering	Number of observations	Fraction
fcc(1 1 1)	15	0.58
hcp	4	0.15
Other	7	0.27
Total number of observations	26	1.0

our results. A clear preference for fcc is found, with 65% of the regions of well-defined ordering showing an fcc stacking (ABC).

The terraces at the bottom of the foam sample (at the foam–water interface) can be formed by both triangular layers of bubbles (fcc, hcp or other) or square layers consistent with fcc(1 0 0). We have analysed the stacking sequence of the triangular layers, comparing the positions of the bubble centres of successive layers. Random sampling is not applied here, as it is generally quite difficult to find large terraces perfect enough for analysis of the type shown in Fig. 5.

The advantage of the analysis of the terraces is that often more than three successive layers can be analysed. In nine foam samples, we analysed 43 terraces, of which 26 contained four layers or more. The results of these 26 measurements are shown in Table 2. Here we made the distinction between stackings consistent with fcc (ABCABC), hcp (ABAB) and other possible sequences, ABAC, etc. We found that 58% of the terraces examined correspond to an fcc arrangement. We did not include the fcc(1 0 0) in this terrace analysis, as random sampling was not applied, but its inclusion would make the preference for fcc even stronger.

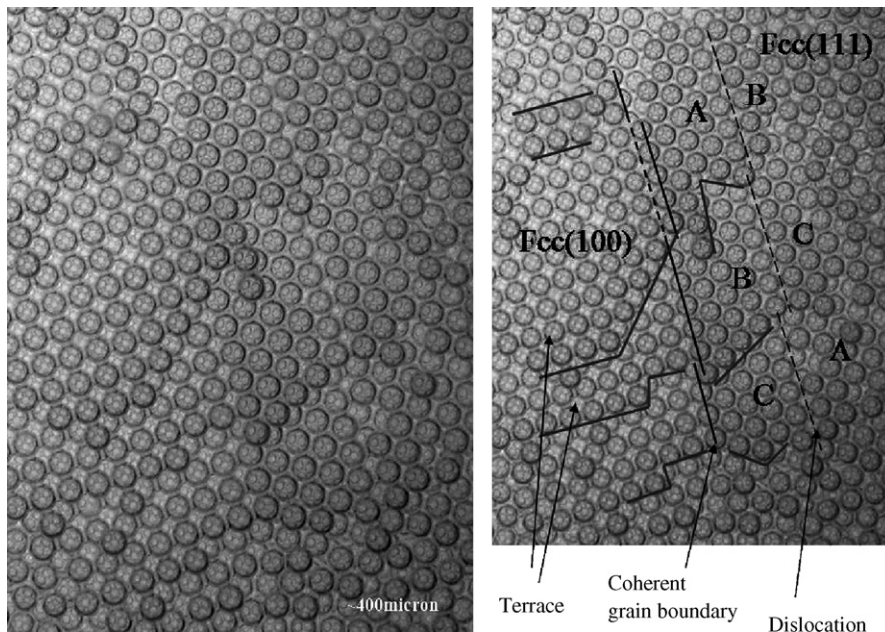


Fig. 6. Terraces, including a coherent grain boundary between fcc(1 0 0) and fcc(1 1 1) and a dislocation at the foam–water interface. Note that such defects can be found as well in metals [37,38].

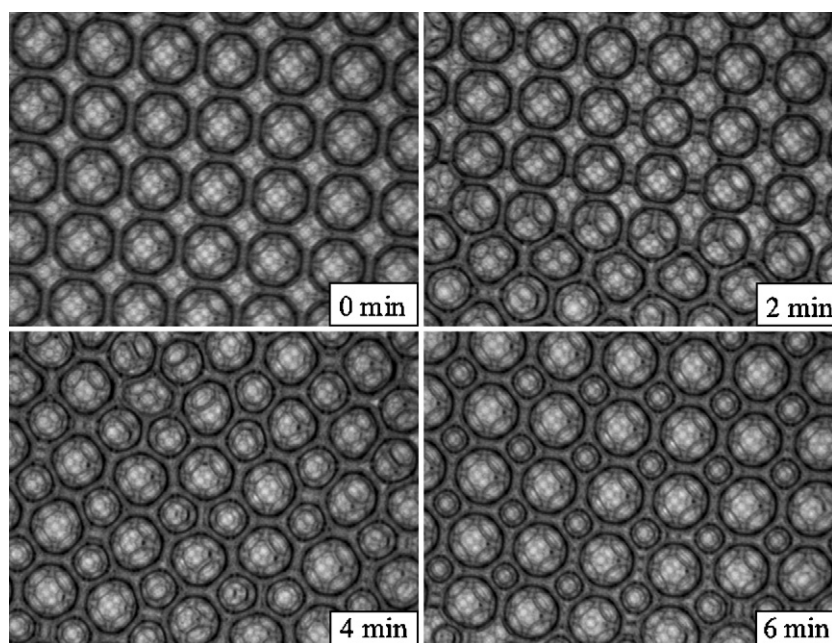


Fig. 7. The modification of the fcc(100) crystal top surface, due to diffusion of nitrogen to the surroundings. After a disordered intermediate stage (2–4 min), a fully ordered bidisperse top layer is formed where the initial surface bubbles fit in the gaps of the next layer (6 min).

5. Self-organising rearrangements due to diffusion at the foam–air interface

In our experiments we have observed that gas (nitrogen) diffusion leads to the elimination of surface layers of bubbles, such that crystalline order is preserved. However, this process proceeds via the creation of a bidisperse top layer as shown in Figs. 7 and 8. The shrinkage of the bubbles in the top layer becomes visible approximately 5 min. After deposition of the foam. It is driven by the pressure difference between the top bubbles and the atmosphere, which greatly exceeds the pressure difference between the bulk bubbles. The shrinkage of bubbles creates space for the bubbles below to move upwards, driven by buoyancy. Initially, this results in a seemingly disordered structure, however, eventually the initial top bubbles shrink so much that they fit into the sites between the bubbles of the original second layer. Surprisingly, in the case of the fcc(100) crystals the structure forms a fully ordered bidisperse top layer at this stage, as can be seen in Fig. 7.

In the case of fcc(111) crystals, a bidisperse top layer is formed in the same manner as for the fcc(100), but since an fcc(111) layer has twice as many possible sites as bubbles, it is not possible to fill all the sites (Fig. 8). So for fcc(111) a *fully ordered* bidisperse top layer can never be formed.

The process of reordering and elimination can continue in the same manner for up to five to six layers and again indicates order in the bulk. The elimination of each layer takes approximately 6 min. This is much quicker compared with the coarsening of a single layer of bubbles on top of a liquid pool, where experiments show that all bubbles are still present after 100 min. This is presumably due to the upward pressure of the layers below, which lifts the bubbles out of the surface. This increases the film area of the top layer and therefore accelerates diffusion.

A similar case of evolving bidispersity out of an initially monodisperse foam was discovered recently in columns of foam, which were produced by continuous bubbling of air through surfactant solution [30]. A full explanation of this still eludes us.

6. Drainage of ordered bubble crystals

Significant drainage occurs in a wet foam if its height exceeds the capillary length [31]. Water flows out of the films and Plateau borders causing the bubbles to eventually deform into polyhedral shapes. For over 100 years it was thought that the most optimal structure for the packing of dry 3D monodisperse bubbles was the Kelvin structure (bcc), in which each bubble is a tetrakaidecahedron, with six 4 sided faces and eight (slightly undulated) hexagonal faces [7]. In 1994 the Weaire–Phelan structure was found to have a slightly lower surface energy. It consists of two types of cells with five and six sided faces [32]. Experimentally only a fragment of this structure has ever been observed [31]. Several layers of the Kelvin structure, however, can form close to a boundary, when the bubbles are confined in a cylinder or between plates; such boundaries are consistent with a (110) plane of the bcc crystal [10,13] and thus assist its formation.

The familiar *bulk* monodisperse dry foams that have been the subject of much research do not readily order, so it is interesting to investigate the drainage of an ordered wet foam as a possible route to creating an ordered dry foam [33]. We have thus considered the drainage of wet bubbles. For this purpose we have made a column of bubbles (diameter $\sim 400 \mu\text{m}$) with a height greater than the capillary length. The foam is confined in a cell consisting of two parallel plates (1 cm \times 5 cm) separated by 3 mm thick rubber strips placed at the sides. The cell is partly open at the bottom so that excess water can drain. The image shown in Fig.

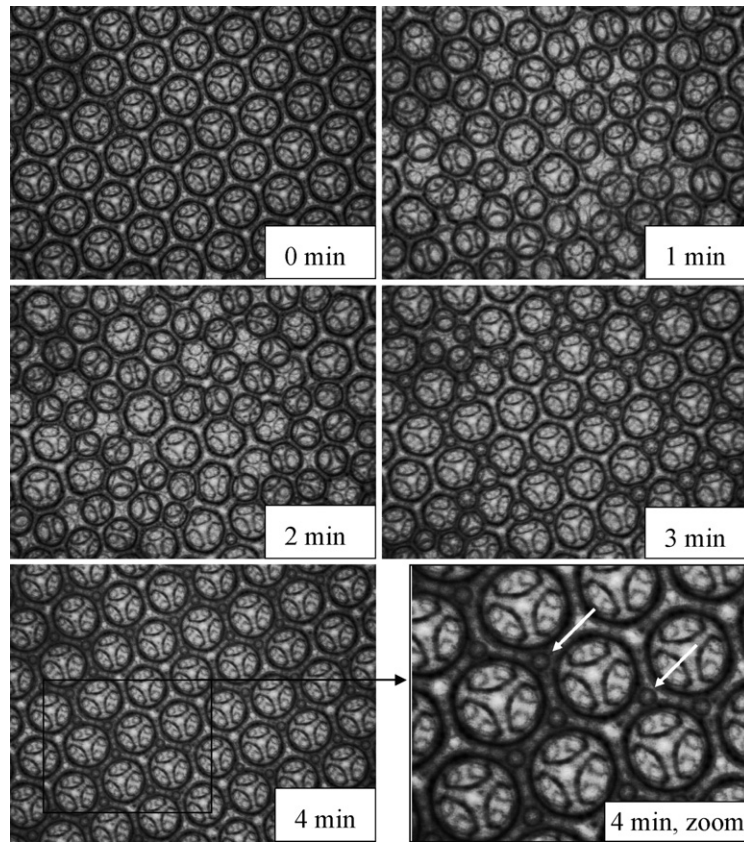


Fig. 8. The modification of the $\text{fcc}(111)$ crystal top surface, driven by diffusion of nitrogen to the atmosphere. After a highly disordered intermediate stage (1–2 min) a bidisperse top layer is formed in which the initial surface bubbles fit in the interstices of the next layer (3–4 min). Compared with the $\text{fcc}(100)$ coarsening (Fig. 7) the bidispersity stage is not as obvious, since the bubbles of the initial top layer are already very small (see arrows) when the ordered stage is reached.

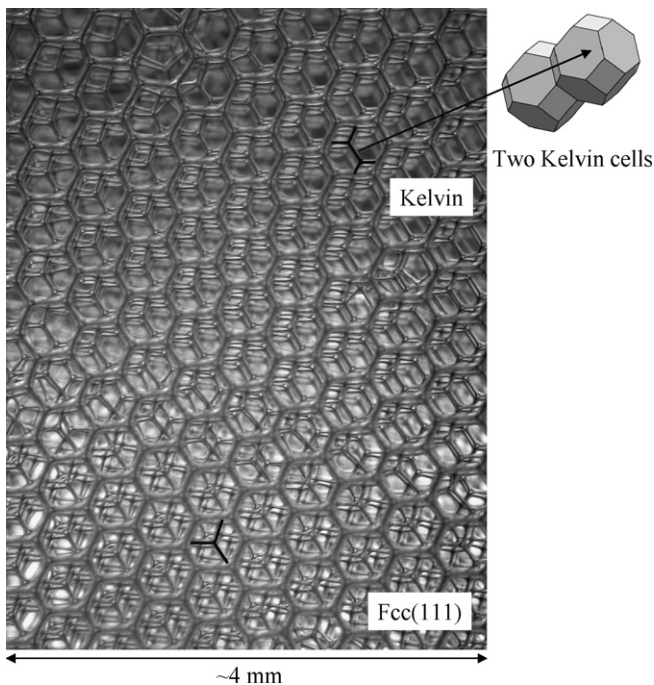


Fig. 9. Drained bubbles in a Hele-Shaw cell (of diameter $400\ \mu\text{m}$). In the upper section the bubbles are arranged in a Kelvin (bcc) packing, at the bottom they are packed according to $\text{fcc}(111)$. A notched ordered interface separates the two crystals.

9 was taken at a height of 2.5 cm. At the top we can see Kelvin cells while at the bottom the foam has an $\text{fcc}(111)$ structure. In future work we will investigate the *dynamics* of the transition from the wet hcp or fcc structure to the dry Kelvin structure, using a high speed camera and image analysis.

In our confined system we can create dry foam composed of an estimated six to eight layers of Kelvin cells in thickness. We are currently investigating how this technique can be adapted to create a larger system of bulk Kelvin cells or indeed whether the Weaire–Phelan structure can be found.

The transition between bcc and fcc is a longstanding point of interest [34]. The bcc structure becomes mechanically unstable when the liquid fraction reaches about 10%. The reverse transition is much more problematic: certainly, extensive hysteresis is expected [31]. The present procedure seems to offer a suitable experimental system for further investigation of these transitions; see also [33,10].

7. Conclusions and outlook

We have extended the structural characteristics of the wet bubble crystals first observed by Bragg and Nye [1]. By using a ray-tracing technique we can distinguish between ABC and ABA packings at the top surface. This method, together with the analysis of terraces at the foam–water interface, was used to

estimate the frequency of occurrence of the crystalline structures of fcc and hcp, at least to the extent that the stacking sequence is followed for several layers, with some corroborative evidence for deeper order. The clear preference for an fcc structure is not yet clearly understood.

We have indicated a particular effect of gas diffusion at the top surface layer, where through a stage of a seemingly disordered surface structure, finally a fully ordered bidisperse top layer for fcc(100) emerges. The process repeats itself for consecutive layers. We also showed preliminary results on the drainage of the wet structures, raising some interesting questions with regards the transition from dry to wet foam and vice versa, and the possibility to search for the Weaire–Phelan structure.

The mechanism by which the bubble system orders is still unclear, but several possible factors have been identified. A strong candidate would appear to be the influence of the extensive shearing involved in the rapid extrusion of the bubbles from the outlet, since shear induced ordering is well known to occur under certain circumstances in emulsions [14,15]. Shear could play a role for the occurrence of fcc(100) at the gas–foam surface, together with hydrodynamic effects.

Another possible explanation may be the natural presence of a template of an ordered bubble layer at the gas–water interface. This can stimulate order in the layers of bubbles that form underneath. Templates in colloids and bead systems have been shown to readily induce order depending on the deposition rate [4,35].

In future experiments we will study this effects by artificially imposing a disordered surface template. We will also consider the effects of varying the surfactant concentration and viscosity, in an attempt to isolate the key ingredients required to generate the observed highly ordered crystal structures.

We have investigated the degree to which templating effects can assist ordering in frictionless sphere systems, by performing numerical simulations of the deposition of spheres onto both triangularly packed and square packed surface layers. The simulations consist of a simple “toy-model” in which we perform a time integration of Newton’s equations of motion with appropriate inter-sphere and sphere–liquid interactions. Spheres introduced at the bottom of our simulation cell filled

with liquid, rise due to buoyancy. Colliding spheres interact via the Hertz law. Dissipative effects are incorporated into the simulations via the inclusion of velocity-dependent Stokes forces and the consideration of viscoelastic dissipation in sphere collisions.

We find a very high degree of ordering in the bulk sphere packing if we initialise the simulations by an ordered (triangular) surface layer of spheres (Fig. 10) [36]. This occurs both for the case where spheres are released at random points at the bottom of the simulation box or at just a single point. The ordering for the latter scenario is generally more perfect.

Acknowledgments

We wish to thank JF Nye for his advice and information on his remarkable early work. R. Höhler and S. Cohen-Addad are thanked for introducing us to their work on similar systems. We gratefully acknowledge stimulating discussions at the EPSRC funded FRIT workshop in Aberystwyth, June 2005 by S. Cox. Our work was supported by the European Space Agency (MAP AO-99-108:C14914/02/NL/SH, MAP AO-99-075:C14308/00/NL/SH), Enterprise Ireland (BRG SC/2002/011) and Science Foundation Ireland (RFP 05/RFP/PHY0016). WD is an IRCSET Postdoctoral Fellow.

References

- [1] L. Bragg, J.F. Nye, A dynamical model of a crystal structure, Proc. R. Soc. Lond. Ser. A: Math. Phys. Sci. 190 (1023) (1947) 474–481.
- [2] J. Nye, Private communication, 2005.
- [3] A. van der Net, W. Drenckhan, D. Weaire, S. Hutzler, The crystal structure of bubbles in the wet foam limit, Soft Matt. 2 (2) (2006) 129–134.
- [4] O. Pouliquen, M. Nicolas, P.D. Weidman, Crystallization of non-Brownian spheres under horizontal shaking, Phys. Rev. Lett. 79 (19) (1997) 3640–3643.
- [5] Y. Nahmad-Molinari, J.C. Ruiz-Suarez, Epitaxial growth of granular single crystals, Phys. Rev. Lett. 89 (26) (2002) 264302.
- [6] O. Carvente, J.C. Ruiz-Suarez, Crystallization of confined non-Brownian spheres by vibrational annealing, Phys. Rev. Lett. 95 (1) (2005) 018001.
- [7] T. Aste, D. Weaire, The Pursuit of Perfect Packing, Institute of Physics Publishing, 2000.
- [8] H. Miguez, F. Meseguer, C. Lopez, A. Mifsud, J.S. Moya, L. Vazquez, Evidence of fcc crystallization of SiO₂ nanospheres, Langmuir 13 (23) (1997) 6009–6011.
- [9] J.X. Zhu, M. Li, R. Rogers, W. Meyer, R.H. Ottewill, W.B. Russell, P.M. Chaikin, Crystallization of hard-sphere colloids in microgravity, Nature 387 (6636) (1997) 883–885.
- [10] M.E. Rosa, M.A. Fortes, M.F. Vaz, Deformation of three-dimensional monodisperse liquid foams, Eur. Phys. J. E 7 (2) (2002) 129–140.
- [11] S. Hutzler, D. Weaire, R. Crawford, Moving boundaries in ordered cylindrical structures, Philos. Mag. B 75 (6) (1997) 845–857.
- [12] S. Hutzler, N. Peron, D. Weaire, W. Drenckhan, The foam/emulsion analogy in structure and drainage, Eur. Phys. J. E 14 (4) (2004) 381–386.
- [13] M.A. Fortes, E. Rosa, Private communication, 2005.
- [14] T.G. Mason, J. Bibette, Shear rupturing of droplets in complex fluids, Langmuir 13 (17) (1997) 4600–4613.
- [15] P. Perrin, Amphiphilic copolymers: a new route to prepare ordered monodisperse emulsions, Langmuir 14 (21) (1998) 5977–5979.
- [16] L.V. Woodcock, Computation of the free energy for alternative crystal structures of hard spheres, Faraday Discuss. 106 (106) (1997) 325–338.

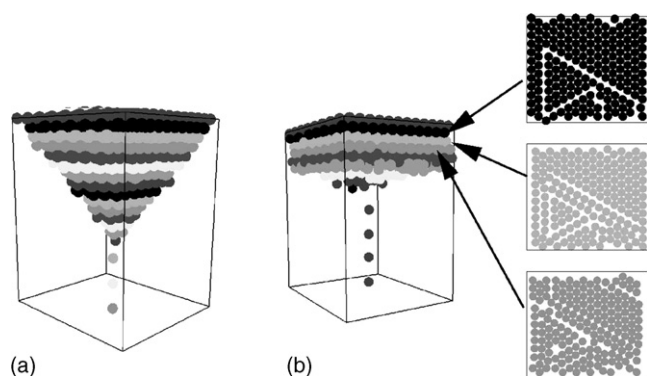


Fig. 10. Simulation of the deposition (from below) of spheres onto a triangularly packed surface layer. The ordering of the balls is controlled by the amount of dissipation in the system. While for low dissipation a large number of defects are generally observed (a), a perfect fcc ordering can be achieved if dissipation is increased (b).

- [17] P.N. Pusey, W. Vanmegen, P. Bartlett, B.J. Ackerson, J.G. Rarity, S.M. Underwood, Structure of crystals of hard colloidal spheres, *Phys. Rev. Lett.* 63 (25) (1989) 2753–2756.
- [18] A. Saint-Jalmes, D. Langevin, Time evolution of aqueous foams: drainage and coarsening, *J. Phys. Condens. Matt.* 14 (40) (2002) 9397–9412.
- [19] A.M. Ganan-Calvo, Perfectly monodisperse microbubbling by capillary flow focusing: an alternate physical description and universal scaling. Part 2, *Phys. Rev. E* 69 (2) (2004) 027301.
- [20] W. Drenckhan, S.J. Cox, G. Delaney, H. Holste, D. Weaire, N. Kern, Rheology of ordered foams—on the way to discrete microfluidics, *Coll. Surf. A: Physicochem. Eng. Aspects* 263 (1/3) (2005) 52–64.
- [21] D. Weaire, W. Drenckhan, Discrete Microfluidics - a review of recent progress, *Adv. Colloid Interface Sci.*, Submitted for publication, 2006.
- [22] A.M. Ganan-Calvo, Generation of steady liquid microthreads and micron-sized monodisperse sprays in gas streams, *Phys. Rev. Lett.* 80 (2) (1998) 285–288.
- [23] P.B. Umbanhowar, V. Prasad, D.A. Weitz, Monodisperse emulsion generation via drop break off in coflowing stream, *Langmuir* 2000 (16) (1999) 347–351.
- [24] A.M. Ganan-Calvo, J.M. Gordillo, Perfectly monodisperse microbubbling by capillary flow focusing, *Phys. Rev. Lett.* 87 (27) (2001).
- [25] J.M. Gordillo, Z. Cheng, A.M. Ganan-Calvo, M. Marquez, D.A. Weitz, A new device for the generation of microbubbles, *Phys. Fluids* 16 (8) (2004) 2828–2834.
- [26] T. Thorsen, R.W. Roberts, F.H. Arnold, S.R. Quake, Dynamic pattern formation in a vesicle-generating microfluidic device, *Phys. Rev. Lett.* 86 (18) (2001) 4163–4166.
- [27] A.S. Utada, E. Lorenceau, D.R. Link, P.D. Kaplan, H.A. Stone, D.A. Weitz, Monodisperse double emulsions generated from a microcapillary device, *Science* 308 (5721) (2005) 537–541.
- [28] Autodesk. 3d Studio Max, <http://www.autodesk.com/3dsmax>, 2006.
- [29] A. van der Net, L. Blondel, A. Saugey, W. Drenckhan, Simulating and interpreting images of foams with computational ray-tracing techniques, *Coll. Surf. A: Physicochem. Eng. Aspects* 309 (1) (2007) 159–176.
- [30] K. Feitosa, D.J. Durian, Bubble kinetics in a steady-state column of aqueous foam, *Europhys. Lett.* (2006) (Preprint).
- [31] D. Weaire, S. Hutzler, *The Physics of Foams*, Clarendon Press, Oxford, 1999.
- [32] D. Weaire, R. Phelan, A counterexample to Kelvin conjecture on minimal-surfaces, *Philos. Mag. Lett.* 69 (2) (1994) 107–110.
- [33] R. Höhler, Personal communication.
- [34] D. Weaire, S. Hutzler, N. Pittet, Cylindrical packings of foam cells, *Forma* 7 (3) (1992) 259–263.
- [35] A. van Blaaderen, R. Ruel, P. Wiltzius, Template-directed colloidal crystallization, *Nature* 385 (6614) (1997) 321–324.
- [36] G.W. Delaney, Computational studies of the structure and dynamics of packings of grains and bubbles, PhD thesis, Trinity College Dublin, 2006.
- [37] C. Klein, *The Manual of Mineral Science*, 22nd ed., John Wiley and Sons, 1977.
- [38] J.P. Hirth, J. Lothe, *Theory of Dislocations*, 2nd ed., John Wiley and Sons, 1982.